Slowing down supercooled liquids by manipulating their local structure: Supplementary Information

Susana Marín-Aguilar, Henricus H. Wensink, Giuseppe Foffi, and Frank Smallenburg
Laboratoire de Physique des Solides, CNRS, Université Paris-Sud, Université Paris-Saclay, 91405 Orsay, France
(Dated: November 4, 2019)

STRUCTURE ANALYSIS

Bond Order Parameters

The structural analysis made with the Topological Cluster Classification (TCC) [1] algorithm was supported by the information given by the local bond order parameters Q_6 and $\hat{W}_6$ [2, 3].

Local bond order parameters characterize the environment of each particle, based on its nearest neighbors. We assign to each particle i a bond-order vector Q_{lm}, which contains the expansion of its local environment in terms of spherical harmonic functions of order l. To measure the local bond-order vector Q_{lm}, a list of neighbors is constructed for each particle, containing all other particles within a radial distance $r_c = 1.2\sigma_L$. We denote the number of neighbors for particle i as $N_b(i)$. For each particle i, $Q_{lm}(i)$ is then given by

$$Q_{l,m}(i) = \frac{1}{N_b(i)} \sum_{j=1}^{N_b(i)} Y_{lm}(\theta_{ij}, \phi_{ij}), \tag{S1}$$

where $Y_{lm}(\theta, \phi)$ are the spherical harmonics, with $m \in [-l, l]$ and θ_{ij} and ϕ_{ij} are the polar and azimuthal angles of the center-of-mass distance vector $\mathbf{r}_{ij} = \mathbf{r}_j - \mathbf{r}_i$, with $\mathbf{r}_i$ the position vector of particle i.

The invariants used to characterize the local structures are rotationally invariant combinations, such as:

$$Q_l = \left[\frac{4\pi}{2l+1} \sum_{m=-l}^{l} |\langle Q_{lm}(\mathbf{r}) \rangle|^2 \right]^{1/2}, \tag{S2}$$

and

$$W_l = \sum_{m_1, m_2, m_3, m_1+m_2+m_3=0} \begin{pmatrix} l & l & l \\ m_1 & m_2 & m_3 \end{pmatrix} \langle Q_{lm_1} \rangle \langle Q_{lm_2} \rangle \langle Q_{lm_3} \rangle, \tag{S3}$$

where the coefficients in the matrix in W_l corresponds to the Wigner $3j$ symbols[4]. The W_l commonly used are the ones normalized as

$$\hat{W}_l = W_l / \left[\sum_{l=-m}^{m} |\langle Q_{lm}(\mathbf{r}) \rangle|^2 \right]^{3/2}. \tag{S4}$$

The FCC (face-centered-cubic), HCP (hexagonal-closed-packing) and icosahedral clusters each correspond to specific values of the bond order parameters that allow us to distinguish them. An suitable choice for identifying icosahedral clusters is via Q_6 and $\hat{W}_6$, that have values of $Q_6 = 0.663$ and $\hat{W}_6 = -0.170$ each for a perfect icosahedral cluster. These values provide a reference point for finding icosahedral structure in the supercooled liquid. We classify all particles whose environment is sufficiently similar to this ideal cage (i.e. $Q_6 > 0.5$ and $\hat{W}_6 < -0.1$) as icosahedral particles, as illustrated in the inset of Fig. S1. We then plot in Fig. S1 the fraction N_{ico}/N of icosahedral particles in the system as a function of temperature for different patch geometries. The corresponding results are in good agreement with the ones shown in Fig. 5b in the main text, demonstrating that the details involved in identifying icosahedral cluster do not impact our results.

To illustrate the trends found with the local bond order parameters in Fig. S2, we show scatterplots of $\hat{W}_6$ and Q_6 [2, 3] for different patch geometries at a temperature of $k_BT/\epsilon = 0.4$, with k_B Boltzmann's constant, T the temperature, and ϵ the bonding energy. The red dots indicate the order parameter values for a perfect icosahedral cage. The 12-patch system shows a clear preference for icosahedral order in comparison to the other systems.

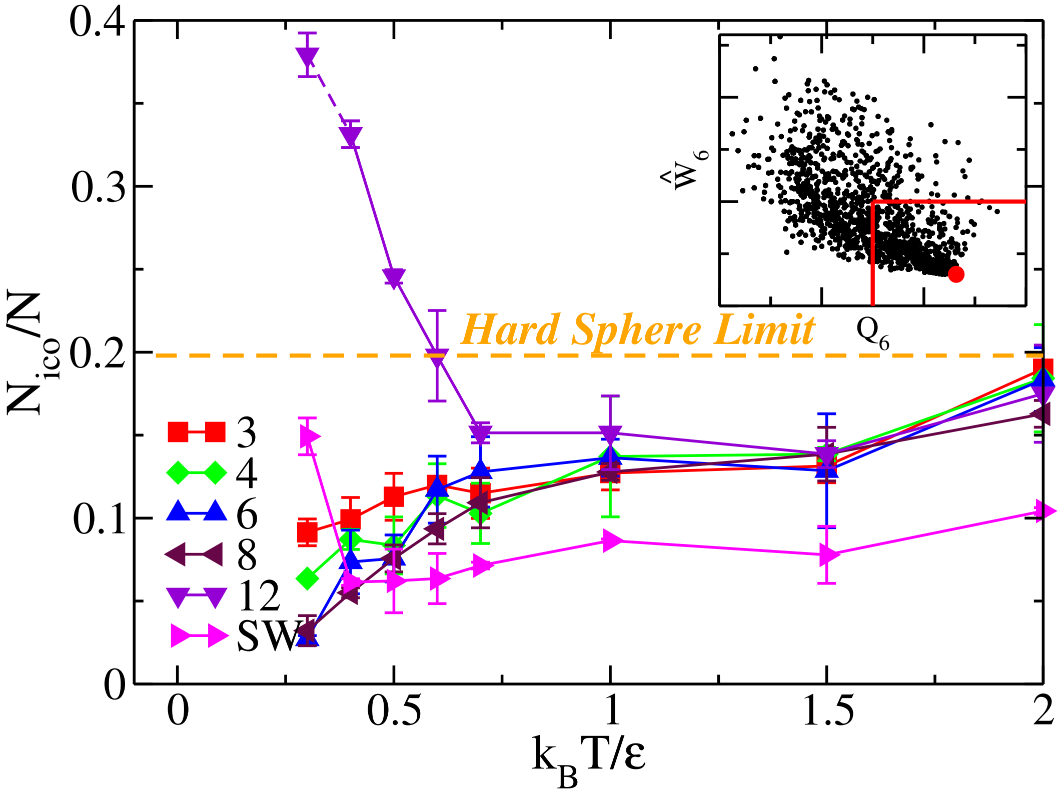

FIG. S1. Fraction of particles in a local environment with icosahedral order, as a function of temperature and patch geometry. The dashed horizontal line indicates the value in the hard-sphere limit. The inset shows a plot of the bond order parameters Q_6 and $\hat{W}_6$ for individual 12-patch particles at $k_BT/\epsilon = 0.3$, with the red dot indicating the values corresponding to a perfect icosahedral cage. The particles in the region delimited by the red lines are considered to be in an icosahedral environment.

The 12-patch system especially favors the icosahedral environment at low temperatures as also found in our analysis with TCC. Figure S3 shows plots of the bond-orientational order parameters of the 12-patch system through a wide range of temperatures, showing a considerable increase of the number of icosahedral cages at lower temperatures.

Structure Factor

In Fig. S4 we show the structure factor $S(q)$ of a few of the different geometries explored at different temperatures. For all cases shown here, the structure factor remains consistent with a disordered liquid structure, and we see little evidence of change in the local ordering. Hence, we conclude that the structure factor is not a good indicator of the changes in local structure that are associated with local icosahedral ordering.

Analyzed Topological Cluster Classification (TCC) structures

Here, we list the different types of clusters analyzed in this work.

Defective and perfect icosahedra: As mentioned in the main text, the emergence of icosahedral clusters (13A) correlates with the appearance of related structures, such as defective icosahedra (10B), which can similarly be detected using TCC [1]. In Fig. S5a we show a typical defective icosahedral cluster. This cluster is composed of ten particles, and is closely related to the perfect icosahedron shown in Fig. S5b. In Fig. S5f we show the fraction of particles $N_{\rm Dico}$ involved in a defective icosahedral cage. The dependence of $N_{\rm Dico}$ on the temperature is extremely similar to the behavior of the full icosahedra, indicating that these two local motifs are strongly correlated.

Clusters corresponding to crystal lattices: Additionally, the TCC detects clusters corresponding to various crystalline lattices. In Fig. S5 c) we show the cluster corresponding to the body-centered cubic crystal (9X). This

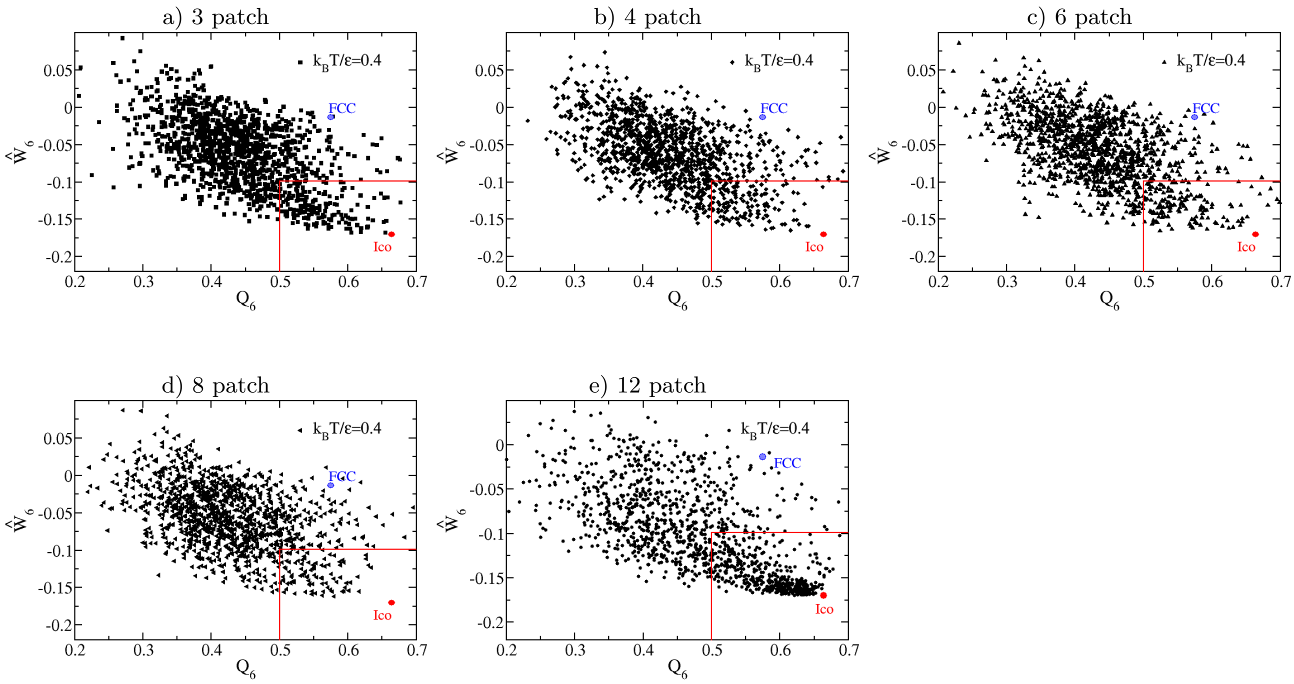

FIG. S2. Bond order parameters Q_6 and $\hat{W}_6$ of each particle for a $k_BT/\epsilon = 0.4$ for the **a)** 3-patch system, **b)** 4-patch system, **c)** 6-patch system, **d)** 8-patch system, **e)** 12-patch system. The bond order parameters for the perfect icosahedral (red) environment and the FCC lattice (blue) are also shown. In all systems, the number of particles $N = 700$, the patch coverage fraction $\chi = 40\%$, and the packing fraction $\eta = 0.58$.

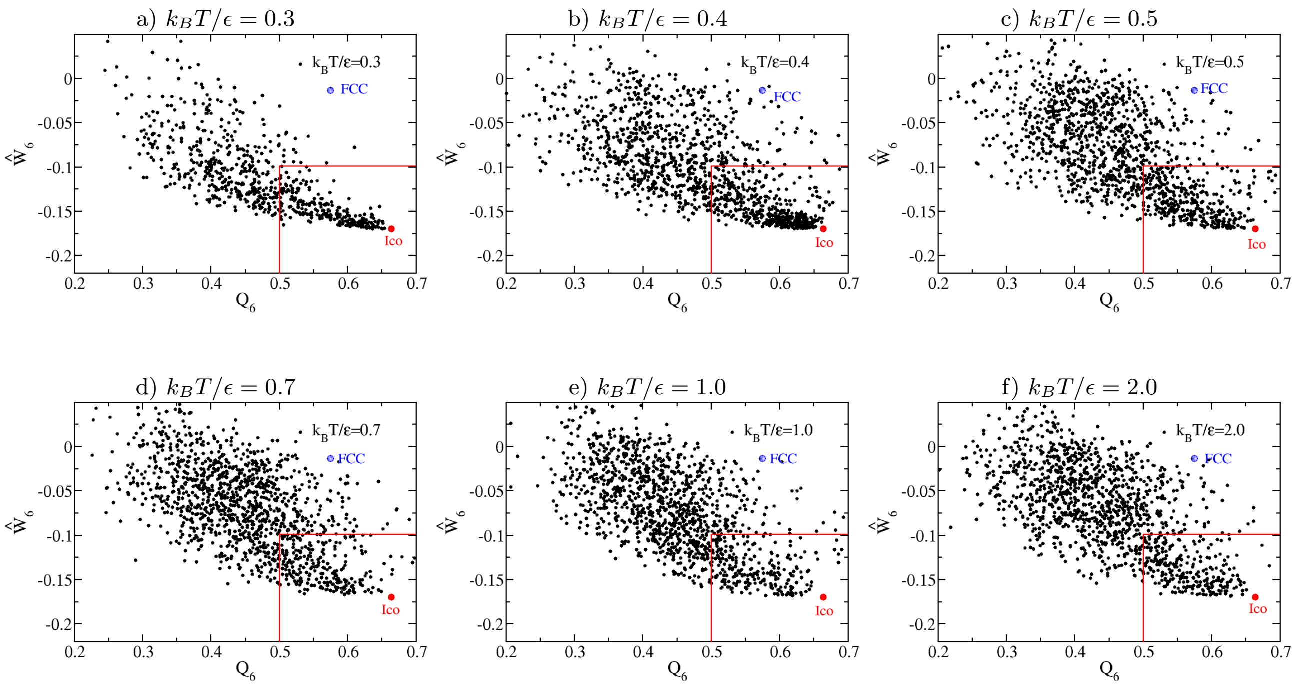

FIG. S3. Bond order parameters of the local environment of each particle of 12-patch systems at different temperatures, **a)** $k_BT/\epsilon = 0.3$, **b)** $k_BT/\epsilon = 0.4$, **c)** $k_BT/\epsilon = 0.5$, **d)** $k_BT/\epsilon = 0.7$, **e)** $k_BT/\epsilon = 1.0$ and **f)** $k_BT/\epsilon = 2.0$. In all systems, the number of particles $N = 700$, the patch coverage fraction $\chi = 40\%$, and the packing fraction $\eta = 0.58$.

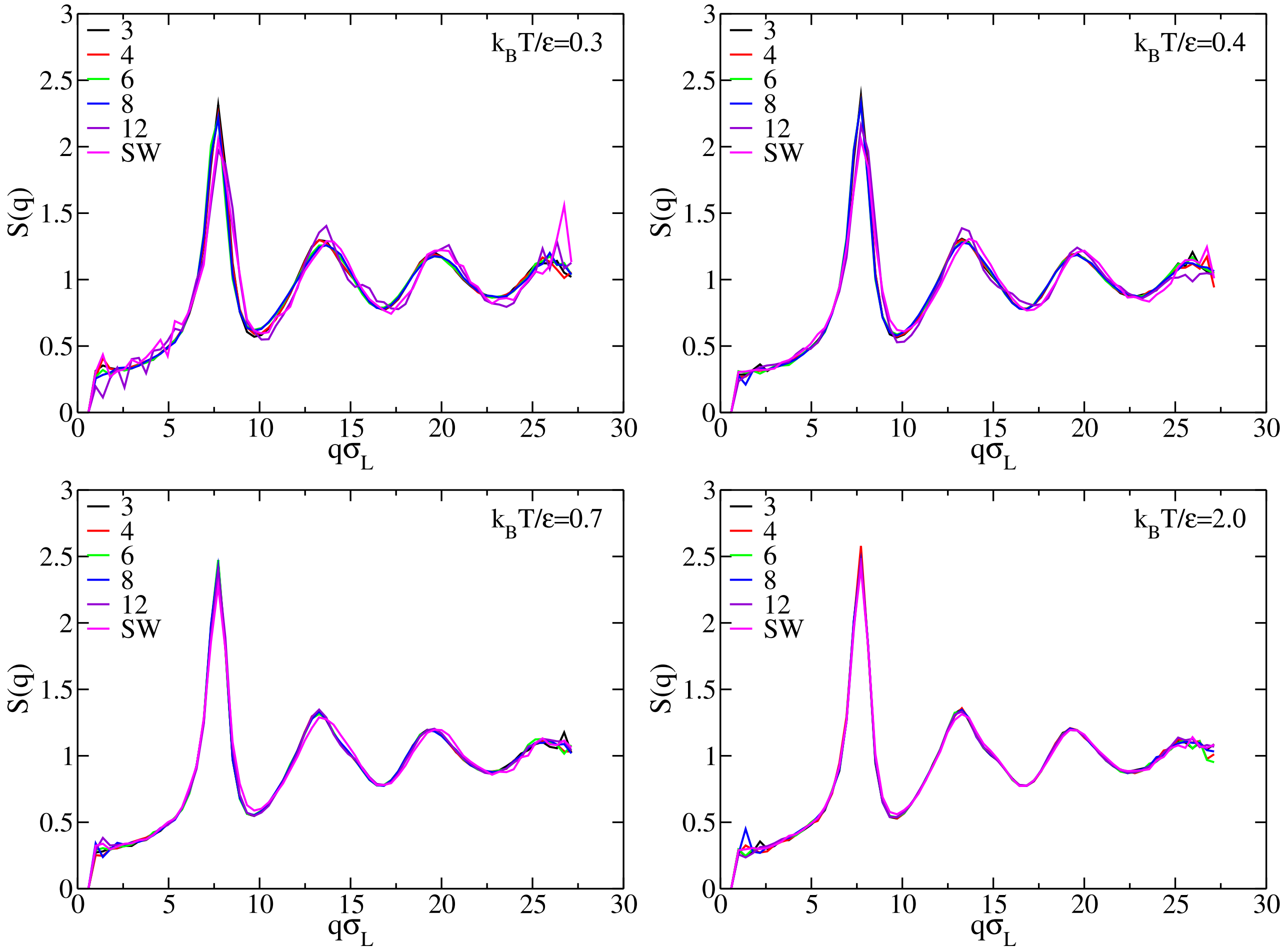

FIG. S4. Structure factor $S(q)$ for patchy systems at different temperatures: **a)** $k_BT/\epsilon = 0.3$, **b)** $k_BT/\epsilon = 0.4$, **c)** $k_BT/\epsilon = 0.7$, **d)** $k_BT/\epsilon = 2.0$. For all cases, the packing fraction $\eta = 0.58$, and the patch coverage fraction $\chi = 40\%$.

cluster is present in all fluids and it is not an indication of crystallization by itself. Fig. S5 d) and e) show the clusters corresponding to a face-centered cubic crystal and hexagonally close-packed crystal, respectively. These last two clusters are essentially absent in the supercooled liquids systems, unless crystallization takes place.

DYNAMICS ANALYSIS

All dynamical quantities reported on the main text correspond to the large particles only. For the small particles, dynamics are faster due to the size of the particle, but the behavior is qualitatively the same. To demonstrate this, we show in Fig. S6 the translational diffusion coefficient of the 6-patch case and 12-patch case respectively for two different coverage χ. The reentrant behavior found for the smaller particles is qualitatively the same as for the larger particles in all cases.

Density Correlation

The shape of the density correlators $F(q,t)$ is dependent on the length of the chosen wavevector $\mathbf{q}$. In Fig. S7 we show some examples of the dependence of the density correlators on the wave vector. Specifically, we plot $F(q,t)$ for two wavelengths below the first peak of the structure factor $S(q)$, the first peak of $S(q)$ and two above the first peak. We show the results for the 6-patch and 12-patch case at $k_BT/\epsilon = 0.4$ and $k_BT/\epsilon = 0.7$.

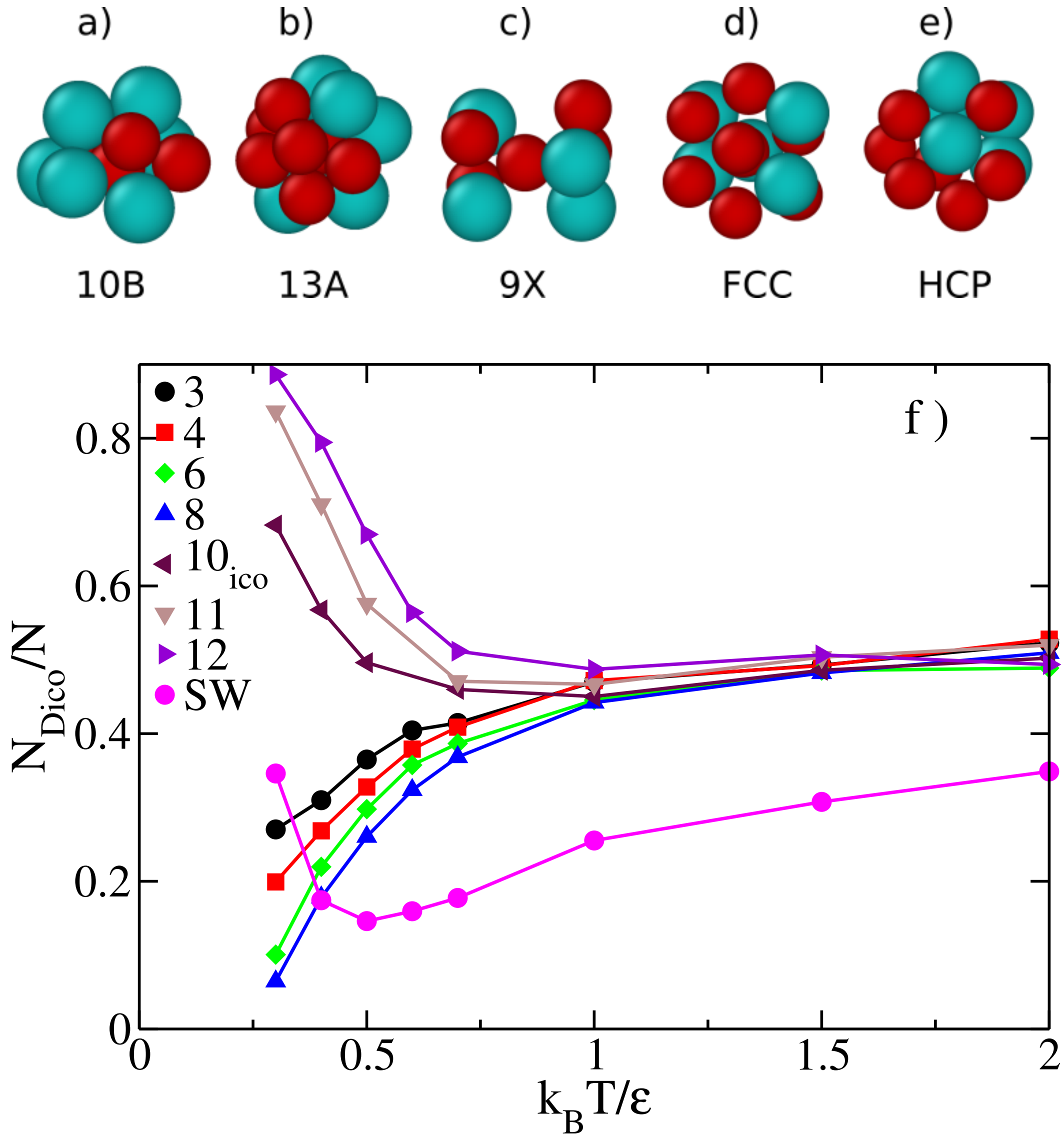

FIG. S5. First row shows typical examples of different cluster types found by TCC: **a)** defective icosahedron, **b)** perfect icosahedron, **c)** cluster 9X corresponding to the BCC lattice, **d)** FCC cluster and **e)** HCP cluster. **f)** shows the fraction of particles in defective icosahedral clusters as a function of temperature for different patch numbers.

[1] A. Malins, S. R. Williams, J. Eggers and C. P. Royall, *J. Chem. Phys.*, 2013, **139**, 234506.
[2] P. J. Steinhardt, D. R. Nelson and M. Ronchetti, *Phys. Rev. B*, 1983, **28**, 784.
[3] Y. Wang, S. Teitel and C. Dellago, *J. Chem. Phys.*, 2005, **122**, 214722.
[4] D. Landau and E. M. Lifshitz, *Quantum Mechanics Non-rekativistic Theory*, Pergamon, 1965, vol. 3.

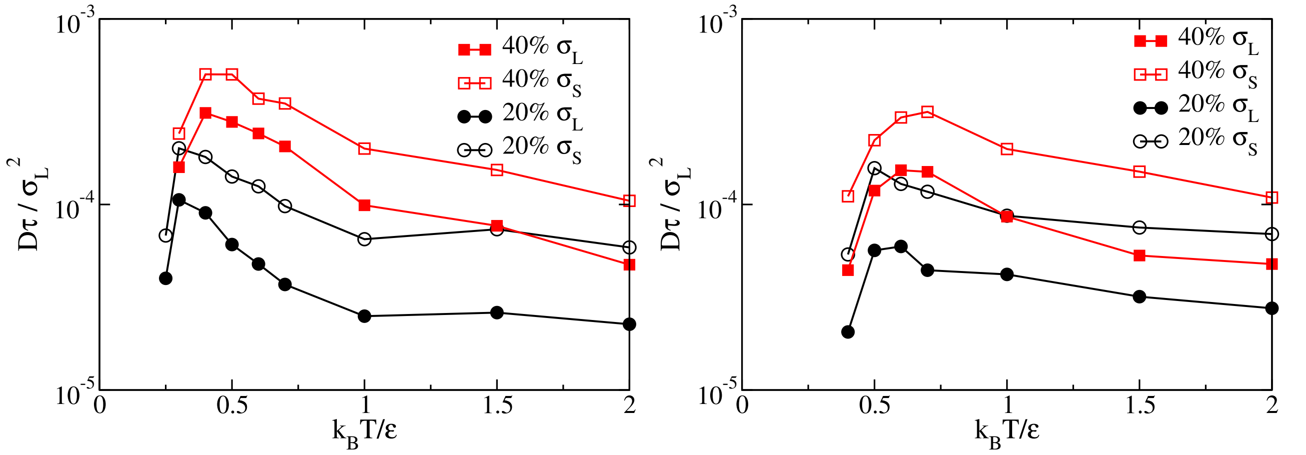

FIG. S6. Translational diffusion coefficients of 6-patch (**a**) and 12-patch (**b**) systems, for both species of particles. Open symbols correspond to the smaller particles.

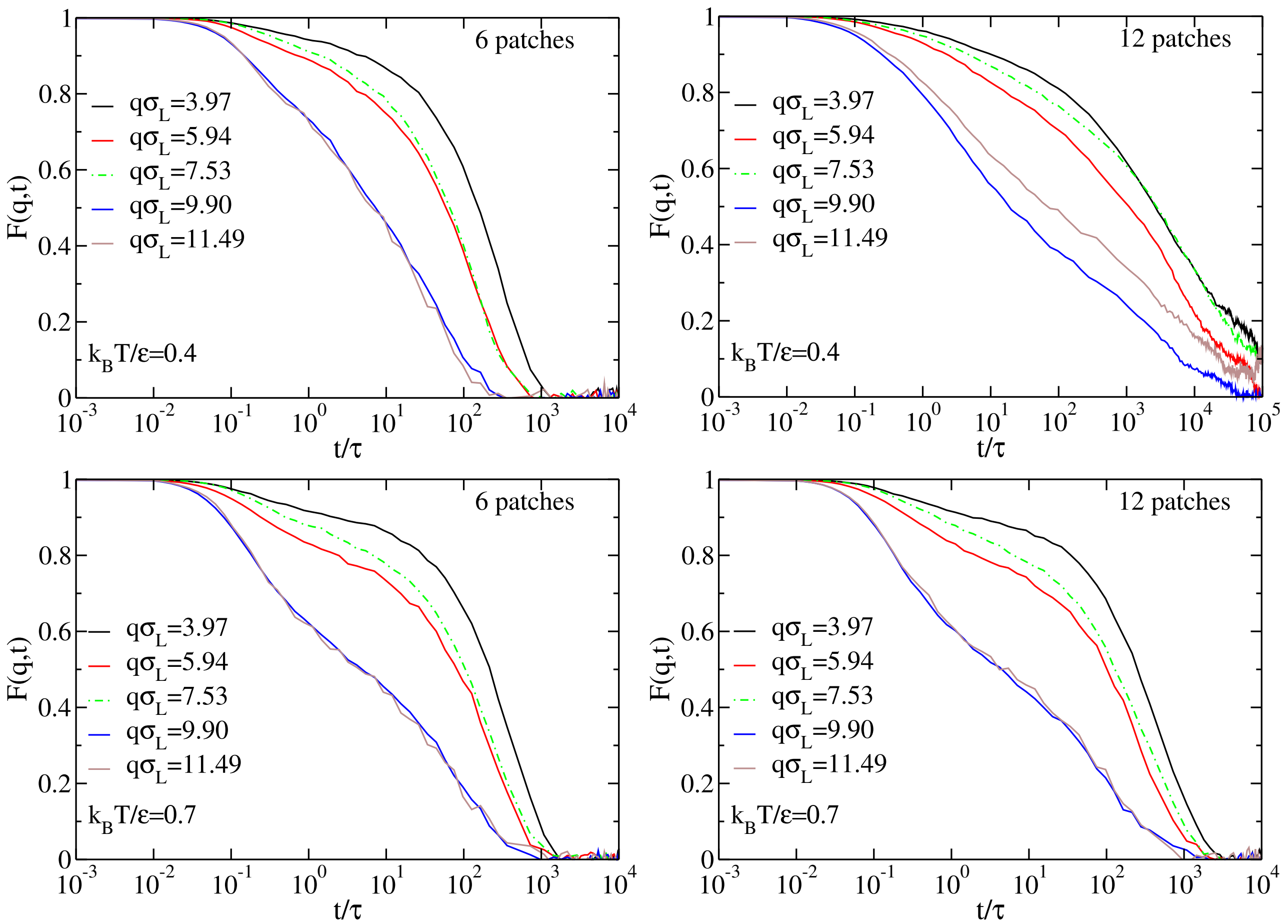

FIG. S7. Density correlation functions at different wavelengths for different patchy systems. In each panel, the green dashed line corresponds to the first peak of the structure factor S(q). **a)** 6-patch case, $k_BT/\epsilon = 0.4$, **b)** 12-patch case, $k_BT/\epsilon = 0.4$, **c)** 6-patch case, $k_BT/\epsilon = 0.7$, **d)** 12-patch case, $k_BT/\epsilon = 0.7$.